Precipitable Water Vapor observation using CLAS augmented signal with a view to real-time estimation

Junichi Takiguchi [1*], Yuichiro Tsukamoto[2], Mikiko Fujita[3]

[1]Dupty General Manager, Innovative Positioning Solutions Marketing and Business Development Dept., Defense & Space Systems Group Mitsubishi Electric Corporation, Japan

[2]Researcher, Quasi-Zenith Satellites Application Section Space Systems Dept.,

Mitsubishi Electric Corporation Kamakura Works, Japan

[3]Senior Scientist, Japan Agency for Marine-Earth Science and Technology, Japan

* Takiguchi.Junichi@dp.mitsubishielectric.co.jp

***Abstract*:** Centimeter Level Augmentation Service (CLAS) is a service that transmits positioning augmentation information to obtain centimeter-level positioning accuracy, and has been transmitted from Quasi-Zenith Satellite System (QZSS), "Michibiki" since November 2018. In this study, we used the next-generation CLAS reinforcement signal developed by Mitsubishi Electric Corporation to estimate and evaluate the accuracy of GNSS Precipitable Water Vapor (GNSS-PWV) with a view to real-time estimation. A special observation network was set up around the Kagoshima Local Meteorological Observatory and observations were conducted in 2022 and 2023. For positioning calculations and atmospheric delay estimation, the tropospheric delay that could not be excluded using the Saastamoinen model or CLAS augmentation information is estimated simultaneously with the user position during precise independent positioning, thus the spatial non-uniformity within the CLAS ionospheric and tropospheric correction grid is addressed. The GNSS-PWV was in agreement with the PWV obtained from radiosondes, with a root mean square error of 3.5 mm The variation in error is comparable to that of GNSS PWV on a moving body estimated by the Final Ephemeris (Fujita et al., 2020), and is relatively large for a fixed point. The bias factors were identified and it was found that the phase correction between the satellite antenna frequencies, the refinement of the receiver antenna parameter, the refinement of the Earth's solid tide model, and the re-estimation of coordinate values were error sensitive. Challenges for real-time implementation and its accuracy evaluation is also reported. We describe the configuration and evaluation of an experimental system that implements JAVAD 4-frequency antenna, CLAS compatible multi-GNSS receiver “AQLOC”, temperature barometer, and the above-mentioned positioning algorithm for CLAS to obtain PWV at one-minute intervals by batch processing.

Keywords: GNSS, QZSS, CLAS, PPP-RTK, PWV, AQLOC-Light

Introduction

In recent years, there have been many linear precipitation system, in which heavy rain continues for several hours or more, causing serious damage such as river flooding and landslides, and the development of technology to accurately predict the amount of rain caused by linear precipitation bands up to several hours in advance is an urgent social issue. In this study, we aim to develop a real-time GNSS–PWV estimation technology that uses the QZSS CLAS and a CLAS-compatible receiver to observe the amount of water vapor before cumulonimbus clouds begin to form. As a positioning reinforcement infrastructure, CLAS has a service area of 800,000 km^2 including the Japanese mainland and territorial waters, and distributes ionospheric and tropospheric corrections on a grid basis in addition to satellite-related corrections such as satellite orbits and clocks. Therefore, by combining it with a CLAS-compatible receiver, it can contribute to improving the spatial density and update interval of GNSS–PWV estimation nationwide.

1. CLAS overview

CLAS is Nation-wide satellite-based augmentation service for PPP-RTK that transmits positioning augmentation information to obtain centimeter-level positioning accuracy, and has been transmitted from the quasi-zenith satellite "Michibiki" since November 2018. Figure 1 shows the CLAS overview. CLAS is “Open service” in Japan with no subscription cost and the operational service is guaranteed by Japanese government for 15 years starts from Q2 2018.

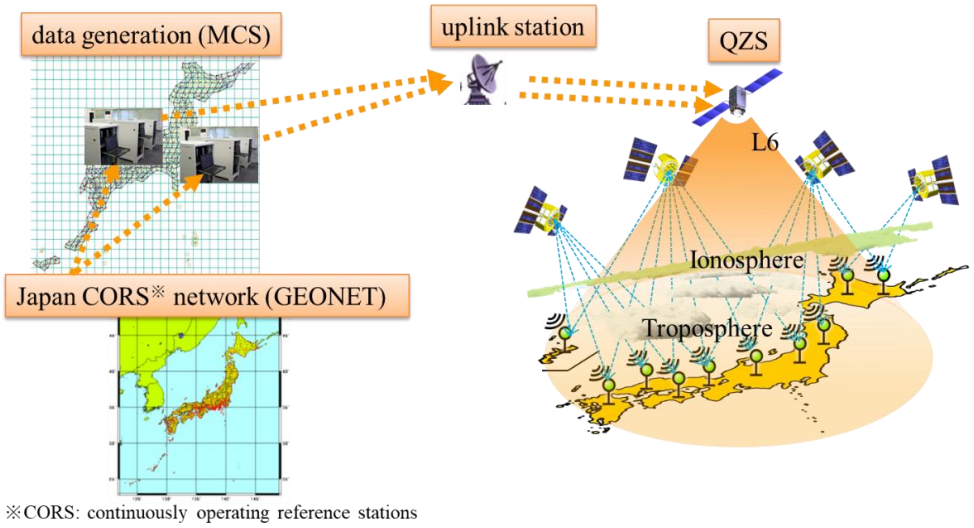

Figure 1: CLAS overview.

Item	Specification

GNSS/Signal	GPS: L1CA, L1C, L2P, L2C, L5 QZS: L1CA, L2C, L5 Galileo: E1B, E5a GLONASS(CDMA): L1OS, L2OS
Area	Japan with territorial waters (800,000 km^2)
Positioning Accuracy (Static)	Horizontal 6cm (95%) Vertical 12cm (95%)
Time to First Ambiguity Fix	<=60[s] (95%)
Service Availability	>=0.99 (constellation) >=0.97 (satellite) >=0.92 (high elevation(60deg))

Table 1: CLAS specification as GNSS augmentation service.

Source: IS-QZSS -L6-005

CLAS is nation-wide satellite-based augmentation service for PPP-RTK. Each error values are separately transmitted based on each dynamics, thus transmitting bandwidth is reduced considerably (<=2,400bps) as shown in Figure 2.

CLAS adopted a method that uses a global network to estimate the state in the order of orbit clock and atmospheric delay. Reinforcement information can be generated stably regardless of whether the ionosphere is quiet or disturbed, making real-time positioning using the PPP-RTK method possible.

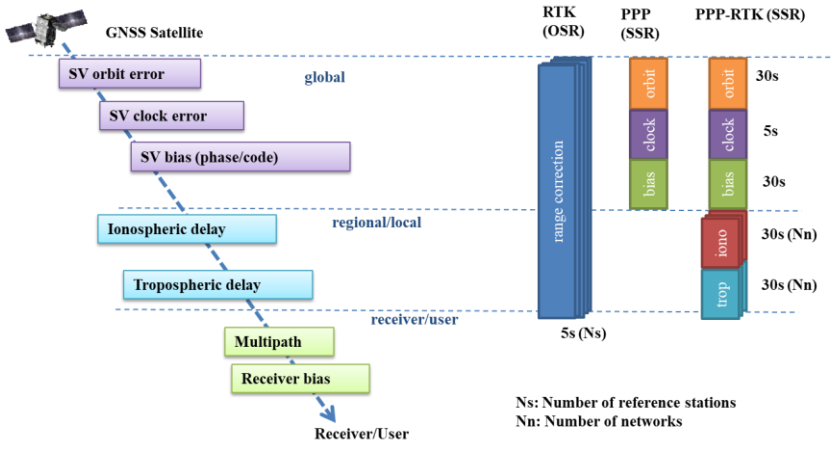

Figure 2: Concept of State-Space Representation (SSR).

2. Tropospheric delay estimation algorithm using CLAS

Ionospheric and tropospheric delays for CLAS reinforcement are provided on a grid collection (delay for ellipsoid height 0m) as shown in Figure 3.

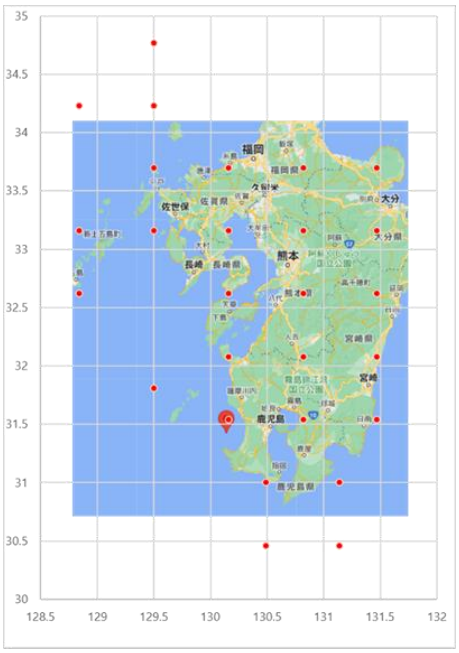

Figure 3: CLAS Tropospheric delay distribution GRID around "Kagoshima".
Source: 4.1.4. Definition of GRID, is-qzss-l6-005

At first, 4 or 3 reference grids with a valid troposphere vertical delay surrounding the user's rough position are selected. The hydrostatic vertical delay $T_{k,hs\,(t)}$ and wet vertical delay $T_{k,wet\,(t)}$ at time t at a selected GRID k are computed by using the troposphere hydrostatic vertical delay variation $\Delta T_{k,hs\,(t)}$ and wet vertical delay variation $\Delta T_{k,wet\,(t)}$ in the compact SSR gridded correction message. δ_{hs0} is Troposphere Vertical delay hydrostatic variation constant value (= 2.3) [m] and δ_{wet0} is Troposphere Vertical Delay Wet Variation constant value (sub type 9: 0.252 [m] + sub type 12: Troposphere residual offset).

$$T_{k,hs\,(t)} = \Delta T_{k,hs\,(t)} + \delta_{hs0} \tag{2.1}$$

$$T_{k,wet(t)} = \Delta T_{k,wet(t)} + \delta_{wet0} \tag{2.2}$$

The rough position is obtained from the single-point positioning. For interpolation or extrapolation with three grids, the weighting coefficient W_k obtained based on the difference for each grid is computed depending on the distance between user's rough position and the grid position. $T_{z,d}^{clas}$ and $T_{z,w}^{clas}$ are the Zenith Hydrostatic Delay (ZHD) and Zenith Wet Delay (ZWD) corresponding to the exact user position by the CLAS correction.

$$T_{z,d}^{clas} = \sum_{k=1}^{4} W_k \cdot T_{k,hs(t)} \tag{2.3}$$

$$T_{z,w}^{clas} = \sum_{k=1}^{4} W_k \cdot T_{k,wet(t)} \tag{2.4}$$

Furthermore, spatial troposphere non-uniformity within the grid is estimated as a user ZWD: $T_{z,w}^{est}$ at the same time during user precise positioning. ZTD is the total tropospheric delay and is expressed as the sum of ZHD and ZWD. Thus, user position's reconstructed ZTD : $T_{z,T}^{user}$ is

$$T_{z,T}^{user} = T_{z,d}^{clas} + T_{z,w}^{clas} + T_{z,w}^{est} \tag{2.5}$$

The user observation equation for carrier phase is as follows. $L_{user}^{PRN}(\mathrm{t})$ is carrier phase observable [m], $\rho_{user}^{PRN}(\mathrm{t})$ is geometric distance to the satellite, c is speed of light, dt_{user} is receiver clock error, dT_{PRN} is satellite clock error, $I_{user}^{PRN}(\mathrm{t})$ is ionospheric delay, $T_{user}^{PRN}(\mathrm{t})$ is slant tropospheric delay, λ is wave length, N is ambiguity, δ_L denote the observation noise, respectively.

$$L_{user}^{PRN}(\mathrm{t}) = \rho_{user}^{PRN}(\mathrm{t}) + c(dt_{user} - dT_{PRN}) - I_{user}^{PRN}(\mathrm{t}) + T_{user}^{PRN}(\mathrm{t}) + \lambda N + \delta_L \tag{2.6}$$

The observation residual v_{user}^{PRN} (the value obtained by subtracting the model value from the observed amount after the observation update) is calculated as follows. Modifier symbol ˆ stands for model value calculated from state variables after observation update.

Observation residuals include satellite orbit/clock errors, signal delays (phase bias), ionospheric delay errors, multipath errors , etc.

$$v_{user}^{PRN}(t) = L_{user}^{PRN}(\mathrm{t}) - \left\{\hat{\rho} + c\left(\widehat{dt} - \widehat{dT}\right) - \hat{I} + \hat{T} + \lambda\hat{N}\right\} \tag{2.7}$$

Ionospheric free coupling is used to remove the first-order term of ionospheric delay errors included in the L1/ L2/E1/E5 observation residuals. The observation residual with ionospheric free coupling is expressed as $\delta_{user}^{PRN}(t)$, where f_1 is L1/E1 carrier frequency and f_2 is L2/E5 carrier frequency.

$$\delta_{user}^{PRN}(t) = \frac{f_1^2}{f_1^2 - f_2^2} v_{user}^{PRN,f_1}(t) - \frac{f_2^2}{f_1^2 - f_2^2} v_{user}^{PRN,f_2}(t) \tag{2.8}$$

Slant Total Delay(STD) can be modeled by a sum of Slant Hydrostatic Delay (SHD) and Slant Wet Delay (SWD) as well as the tropospheric gradients when the homogeneity and inhomogeneity of troposphere are considered, that is:

$$STD = SHD + SWD \tag{2.9}$$

$$SHD = T_{z,d}^{clas} m_d(EL) \tag{2.10}$$

$$SWD = T_{z,w}^{clas} m_w(EL) + T_{z,w}^{est} m(EL) \tag{2.11}$$

$$m(EL) = m_w(EL)\{1 + cot\, EL\, (G_N^W \cdot cos\, AZ + G_E^W \cdot sin\, AZ)\} \tag{2.12}$$

$m_d(EL)$, $m_w(EL)$ and $m(EL)$ are Niell Mapping Function (NMF) regarding hydrostatic and wet delay. G_N^W and G_E^W are horizontal gradient coefficient parameters in north and east directions related to the wetting delay estimated by user precise positioning.

Thus, user position's reconstructed STD : T_{user}^{PRN} is

$$T_{user}^{PRN} = \text{STD} + \delta_{user}^{PRN} \tag{2.13}$$

Below, ZTD and STD are the reconstructed values for user position.

Example of ZTD, STD, and δ_{user}^{PRN} of private observation point near Kagoshima Local Meteorological Observatory using current CLAS was shown in Figure 4. Colors are randomly assigned to satellites with an elevation mask of 15 degrees or more.

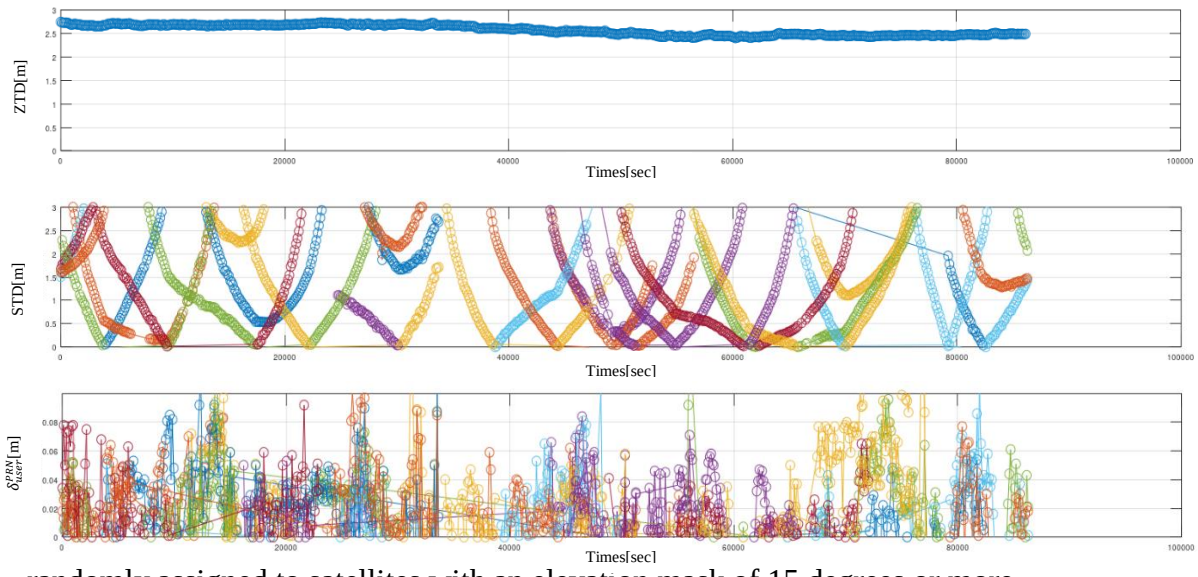

Figure 4: Example of ZTD, STD, and δ_{user}^{PRN}.
00:00:00～23:59:59, 14th June, DOY165, 2023.

3. GNSS observation by a special network

A special observation network was set up around the Kagoshima Local Meteorological Observatory shown in Figure 4. Observations from fixed points were conducted in July 2022 and 2023 using a CLAS-compatible receiver "AQLOC-Light", manufactured by Mitsubishi Electric Corporation and the 4-frequency antenna (GrAnt-G5T manufactured by JAVAD). QZSS (L1C/A, L2C, L6), GPS (L1C/A, L2C), and Galileo(E1, E5b) were received and recorded at 1 sec intervals.

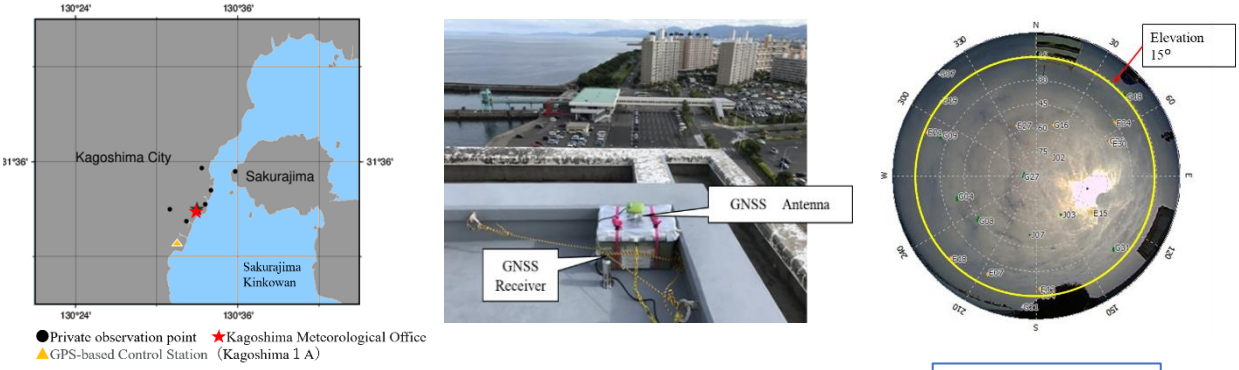

Figure 5: A special observation network.

Figure 6: CLAS compatible Multi-GNSS receiver "AQLOC-Light". (https://www.mitsubishielectric.co.jp/society/space/qzss/aqloc/index.html)

In a ZWD comparison with the F5 solution of the Geospatial Information Authority of Japan GEONET "161218 Kagoshima1A" after post-processing, a root mean square error of 0.029 m and a mean difference of 0.0191 m was obtained, where observation period was 12th to 28th June, DOY163 – DOY179, 2023.

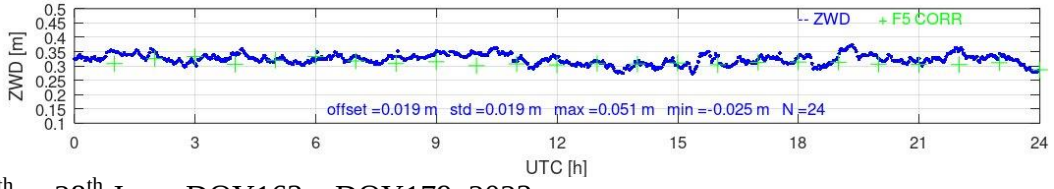

Figure 7: Example of ZWD comparison with GEONET F5 solution

00:00:00～23:59:59, 14th June, DOY165, 2023.

In anticipation of future real-time processing, an experimental system that outputs tropospheric delay estimation results in quasi-realtime by batch processing was constructed. Figure 8 shows a block diagram of the experimental system and its sample log. AQLOC-Light is set to a mode that continuously outputs 1 second observation raw data and CLAS L6 augmentation data. After the stream is input on an industrial PC, the processing window is set every 13 minutes, and after precise positioning, it is compiled into a log file at intervals of 5 minutes and sent to an external PC via Wi-Fi. This transmitted data includes tropospheric delay data as well as temperature and pressure around antenna at the time for ZWD to PWV conversion.

As a result of comparing the post-processing results with the quasi-realtime results, the ZWD difference was a root mean square error of 0.0027 m and the latency was 5~10 minutes as shown in Figure 9.

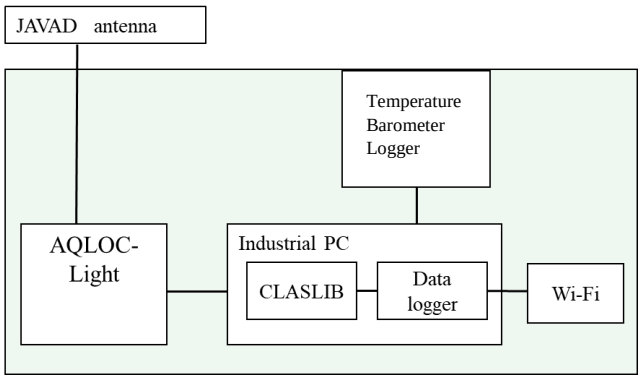


```
#&TROP TOW[s],MJD[d],FIX[1:float 2:fix],ZHD[m],ZWD[m],ZWD est [m],ZTD[m]
$TROP, 430920.0, 60516.987500, 2,  2.3337,  0.2420, -0.0011,  2.5746
$TROP, 430980.0, 60516.988195, 2,  2.3297,  0.2451, -0.0019,  2.5729
$TROP, 431040.0, 60516.988889, 2,  2.3337,  0.2414,  0.0024,  2.5775
$TROP, 431100.0, 60516.989583, 2,  2.3337,  0.2406,  0.0008,  2.5751
$TROP, 431160.0, 60516.990278, 2,  2.3297,  0.2406,  0.0024,  2.5727
$TROP, 431220.0, 60516.990972, 2,  2.3297,  0.2406, -0.0026,  2.5677
$TROP, 431280.0, 60516.991667, 2,  2.3337,  0.2377,  0.0044,  2.5757
$TROP, 431340.0, 60516.992361, 2,  2.3297,  0.2386,  0.0046,  2.5729
$TROP, 431400.0, 60516.993056, 2,  2.3297,  0.2387,  0.0021,  2.5706
$TROP, 431460.0, 60516.993750, 2,  2.3297,  0.2387, -0.0026,  2.5659
$TROP, 431520.0, 60516.994445, 2,  2.3337,  0.2348,  0.0009,  2.5695
$TROP, 431580.0, 60516.995139, 2,  2.3297,  0.2379, -0.0026,  2.5651
$TROP, 431640.0, 60516.995833, 2,  2.3297,  0.2379, -0.0018,  2.5658
$TROP, 431700.0, 60516.996528, 2,  2.3297,  0.2377,  0.0002,  2.5676
```

Updated TRP data

Figure 8: Block diagram of the quasi-realtime tropospheric delay estimation system and its tropospheric output log via WiFi.

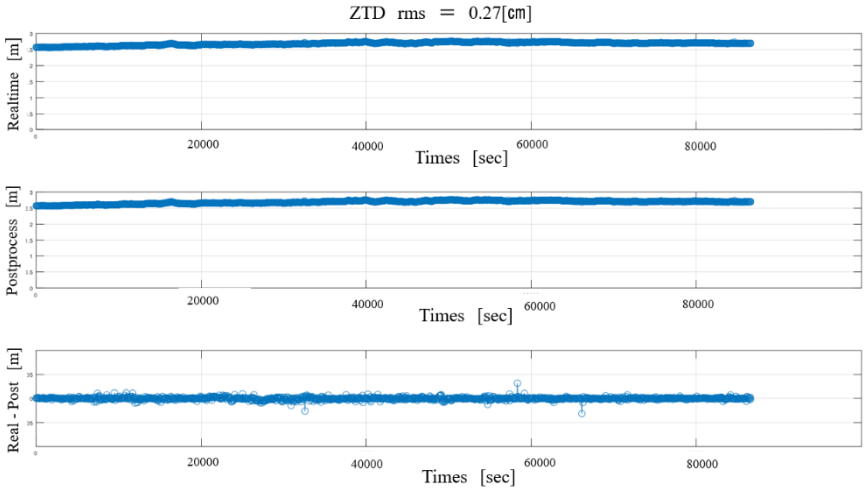

Figure 9 :ZTD difference between Quasi-realtime and post-processing
00:00:00～23:59:59, 26th July, DOY207, 2023.

4. Next generation CLAS

Mitsubishi Electric Corporation has independently developed the next-generation CLAS augmentation signal to improve the current CLAS system. In the next-generation CLAS, the local state variables were decorrelated from the other state variables caused by the satellite as shown in Figure 10. As a result, it became possible to estimate the state variables more robustly even under atmospheric disturbances.

Furthermore, the state quantities of the troposphere and ionosphere can be estimated by making the state quantities closer to the physical quantities, and as a result, convenience and versatility has been improved for application to other applications such as disaster prevention.

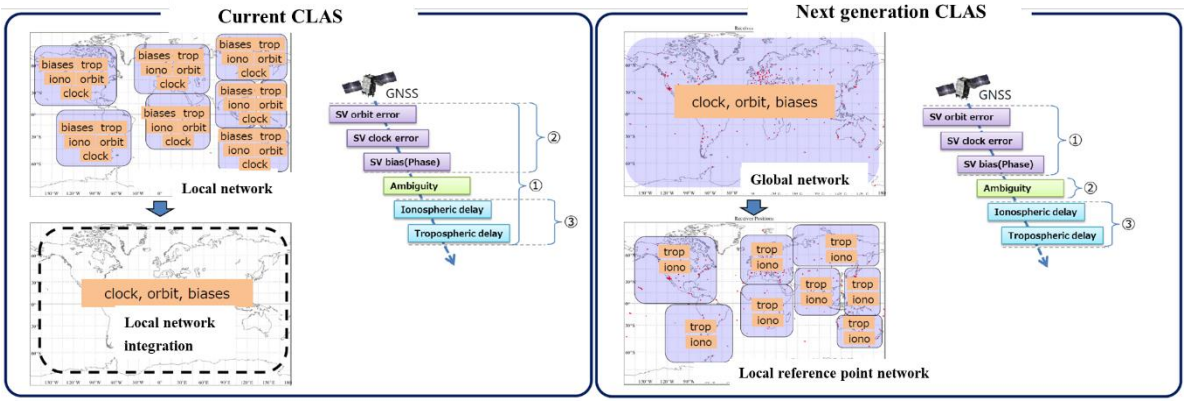

Figure 10 : Comparison of current CLAS and next-generation CLAS methods.

In a ZWD comparison with the F5 solution of the Geospatial Information Authority of Japan GEONET (161218 Kagoshima1A) after post-processing, a root mean square error of 0.0178 m and a mean difference of 0.01 m was obtained, where observation period was 12th to 28th (DOY163 – DOY179) June 2023.

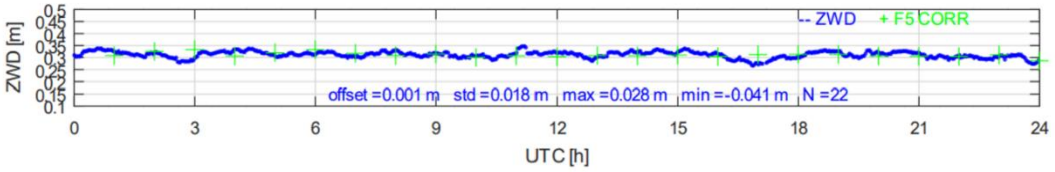

Figure 11: Example of ZWD comparison with GEONET F5 solution
00:00:00～23:59:59, 14th June, DOY165, 2023.

Figure 12 shows the comparison of radiosonde PWV with GNSS-PWV. GNSS-PWV was

the average value for 10 minutes before and after the radiosonde observation time. As a result of the comparison, the error variance was 3.504 mm, and GNSS tended to have a negative bias, -1.935mm .

The error variance was relatively large for a fixed point, equivalent to the GNSS precipitable water mass estimated on a moving object in the final calendar (Fujita et al., 2020), and there was a tendency for the error to be locally large when viewed in a time series.

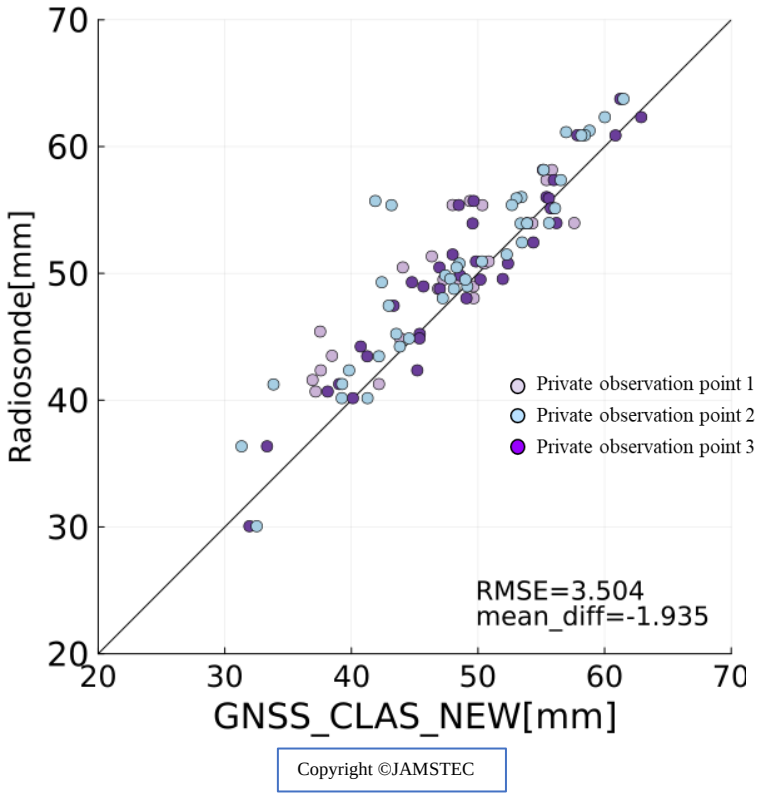

Figure 12: Comparison of Radiosonde PWV with GNSS-PWV (12th June to 28th, 2023)

5. Analysis of mean difference between radiosonde PWV and GNSS-PWV

For the negative mean difference survey of PWV, an approach was taken to reduce the ZTD difference by taking the ZTD of the F5 solution as the true value. By changing 1 to 3 parameters in the Table 1, the absolute value of the ZTD difference and bias polarity for the F5 solution were improved from -0.004 m to 0.001m as shown in Table 3.

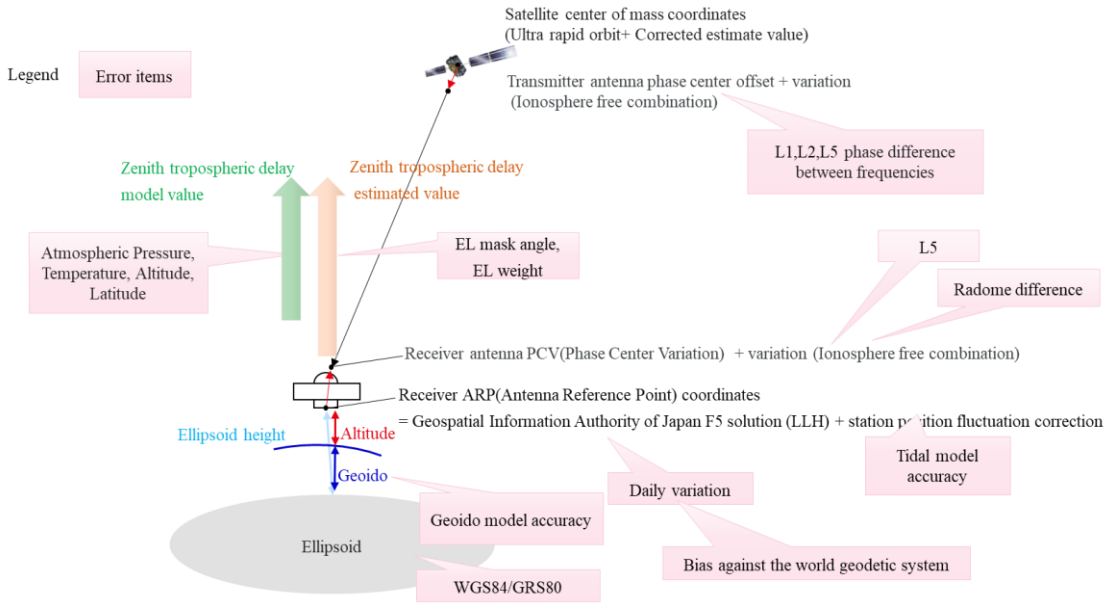

Figure 13: Tropospheric delay error factors.

Table 2: ZTD mean difference influencing factor and parameters.

No	Error factor	Current parameter	Improved parameter
1	Antenna Phase Center Variation (PCV)	NGS	Compatible with antenna radomes at GEONET reference points
2	Earth solid tide model	Simplified model of IERS 1996	IERS Conventions sub-routine (DEHANTTIDEINEL)
3	Phase correction between satellite antenna frequencies	No correction	Correction of L1, L2, and L5
4	Coordinate constraints	Fixed	Fixed

Evaluation	Item	Current parameter	Improved parameter
161218 Kagoshima1A doy176	ZTD mean difference	- 0.004m	0.001m
	ZTD root mean square	0.015m	0.015m

Table 3: ZTD mean difference influencing factor and parameters.

6. Conclusion

In this paper, we report the results of estimating GNSS-PWV using Quasi-Zenith Satellite CLAS and Next-Generation CLAS, and installing a CLAS-compatible multi-GNSS receiver near the Kagoshima Meteorological Observatory. As a positioning augmentation infrastructure, CLAS has a service area of 800,000 km^2 including the Japanese mainland and territorial waters, and distributes ionospheric and tropospheric corrections on a grid basis in addition to satellite-related corrections such as satellite orbits and clocks. Therefore, by combining it with a CLAS-compatible receiver, it can contribute to improving the spatial density and update interval of GNSS precipitable water estimation nationwide.

In a ZTD comparison with the F5 solution of the Geospatial Information Authority of Japan GEONET using current CLAS, a root mean square error of 0.029 m and a mean difference of 0.0191 m was obtained in post-processing. In addition, The ZTD difference between real-time calculation and post-processing calculation was a root mean square error of 0.0027 m and the latency was 5~10 minutes, confirming that no deterioration in accuracy occurred.

In a ZTD comparison with the F5 solution of the Geospatial Information Authority of Japan GEONET using Next-Generation CLAS, a root mean square error of 0.0178 m and a mean difference of 0.010 m was obtained. In addition, the GNSS-PWV was in agreement with the PWV obtained from radiosondes, with a root mean square error of 3.504 mm and a mean difference of -1.935 mm. As a result of analyzing the cause of the bias and its negative polarity, the antenna radome model, the Earth solid tide model, and the L1/L2/L5 antenna phase center were corrected, thus the ZTD mean difference was improved from -0.004 m to 0.001 m.

In the future, we plan to proceed with the development of the next-generation CLAS while exploring the need for high-density, high-temporal frequency GNSS-PWV estimation through Proof of Concept (PoC) demonstration using current CLAS and CLAS-compatible receivers.

References

1. Cabinet Office (Japan), "Quasi-Zenith Satellite System Performance Standard", IS-QZSS-L6-005, 21th Sep.,2022
2. Hirokawa, R., Sato, Y., Fujita, S., and Miya, M., "Compact SSR Message with Integrity Information for Satellite-based PPP RTK Service," Proceedings of 29th International Meeting of the Satellite Division of The Institute of Navigation (ION GNSS+ 2016), Portland, OR, September 2016, pp. 3372-3376.
3. Hiroki Muramatsu, Naofumi Takamatsu, Geodetic Observations Center, (2021). Updating Daily Solution of CORS in Japan Using New GEONET 5th Analysis Strategy. Geospatial Information Authority of Japan Bulletin 2021 No.134
4. Junichi Takiguchi , Yuichiro Tsukamoto, Mikiko Fujita, (2023). GNSS Precipitable Water Vapor observation using CLAS augmented signal. Japan Meteorological Society, Autumn meeting 2023.
5. Mikiko Fujita, Tatsuya Fukuda, Iwao Ueki, Qoosaku Moteki, Tomoki Ushiyama, Kunio Yoneyama, (2020). Experimental Observations of Precipitable Water Vapor over the Open Ocean Collected by Autonomous Surface Vehicles for Real-Time Monitoring Applications. SOLA 16A (Special Edition) 19-24 Nov., 2020
6. RTCM Paper 115-2018-SC104-1071, "Specification of Compact SSR Message for Satellite Based Augmentation Service," Mitsubishi Electric Corporation, RTCM SC-104 meeting, Frankfurt, Germany, October 2018. 6. "CLAS Test Library (CLASLIB)," https://sys.qzss.go.jp/dod/en/downloads/download.html?TECH_ID=36 , August 2018
7. Saito, M., Sato, Y., Miya, M., Shima, M., Omura, Y., Takiguchi, J., and Asari, K., "Centimeter-class Augmentation System Utilizing Quasi-Zenith Satellite System," Proceedings of 24th International Meeting of the Satellite Division of The Institute of Navigation (ION GNSS 2011), Portland, OR, September 2011, pp. 1243-1453.
8. Sato, K., E. Realini,T . Tsuda, M . Oigawa, Y. Iwaki, Y., Shoji and H. Seko, 2013 : A high-resolution, precipitable water vaper monitoring system using a dense network of GNSS receivers. J.DisasterRes., 8, 37−47.
9. Takasu, T, Yasuda, A, "Development of the low-cost RTK-GPS receiver with an open source program package RTKLIB", International Symposium on GPS/GNSS, International Convention Center Jeju, Korea, November 4-6, 2009 8. RTKLIB ver. 2.4.2 Manual, April 29, 2013